Chemical Vapor Deposition and Synthesis on Carbon Nanofibers: Sintering of Ferrocene-Derived Supported Iron Nanoparticles and the Catalytic Growth of Secondary Carbon Nanofibers

Wei Xia,[†] Dangsheng Su,[‡] Alexander Birkner,[§] Lars Ruppel,[§] Yuemin Wang,[†,§] Christof Wöll,[§] Jun Qian,[†] Changhai Liang,[†] Gabriela Marginean,[||] Waltraut Brandl,[||] and Martin Muhler*[,†]

Laboratory of Industrial Chemistry, Ruhr University Bochum, D-44780 Bochum, Germany, Department of Inorganic Chemistry, Fritz Haber Institute of the Max Planck Society, D-14195 Berlin, Germany, Lehrstuhl für Physikalische Chemie I, Ruhr University Bochum, D-44780 Bochum, Germany, and Material Science and Testing, University of Applied Sciences Gelsenkirchen, D-45877 Gelsenkirchen, Germany

Received July 24, 2005. Revised Manuscript Received September 8, 2005

The synthesis of homogeneously distributed carbon nanofibers with well-defined morphology on vapor-grown carbon nanofibers was achieved by a sequence of gas-phase steps, thus fully avoiding wet chemistry: first, carbon nanofibers were exposed to oxygen plasma to introduce oxygen-containing functional groups. Then, the chemical vapor deposition of ferrocene was carried out under oxidizing conditions, yielding nanofiber-supported iron oxide nanoparticles. Secondary carbon nanofibers with diameters in the range from 10 to 20 nm were subsequently grown from cyclohexane catalyzed by the sintered metallic iron nanoparticles under reducing conditions. XPS was applied to monitor the chemical changes of the surface composition and the sintering of the metallic iron particles in hydrogen. The morphology and the height distribution of the sintered iron oxide nanoparticles was derived by a unique combined application of scanning electron microscopy and scanning tunneling microscopy. The specific surface area of the nanocomposite was enhanced strongly due to the growth of secondary nanofibers, and it was possible to tune the morphology of the nanofiber−nanofiber composites by the process parameters. Thus, a significant advance in the reproducible synthesis of branched carbon fiber nanocomposites was achieved.

Introduction

In recent years carbon nanofibers (CNF) and carbon nanotubes (CNT) attracted growing interest in materials science due to their exciting chemical, physical, and mechanical properties.[1] Serp et al.[2] reviewed the application of carbon filaments as catalyst support. Carbon nanofiber- or nanotube-supported transition metal catalysts were used for hydrogenation reactions,[3] in fuel cells,[4] and for other reactions.[5] Mainly surface defects and functional groups can be considered as anchors for metal species.[6] Since the as-synthesized nanofibers or nanotubes do not possess a high density of functional groups or defects on their surface, the filaments are usually functionalized prior to metal deposition.

Branching of carbon fibers was first introduced to overcome the delamination problems in composites by Milewski and co-workers.[7] Downs and Baker[8] improved the process by growing carbon filaments on the surface of polyacrylonitrile(PAN)- and pitch-based carbon fibers via Cu/Ni-catalyzed pyrolysis of C_2H_4. The specific surface area was significantly increased by branching, resulting in an enhanced interfacial bonding between the fibers and the matrix. McAllister and Wolf[9] impregnated Ni on rayon fibers by using the incipient wetness method and grew branches under mild conditions. Recently, Hou and Reneker[10] prepared homogeneously distributed nanofibers grown on PAN-based nanofibers. The iron catalyst used for the nanofiber growth was mixed with the precursor of the PAN fibers, which were then produced by electrospinning. The size of the iron particles ranged from 10 to 30 nm, and the diameter of the secondary nanofibers amounted to about 40 nm.[10] Activated pitch-based carbon fibers were employed as substrates for secondary nanofibers.[11] In addition to the traditional polymer fibers, vapor-grown carbon fibers (VGCFs) were also reported as substrates for the catalytic growth of nanofibers, where the fiber substrate was dipped into a solution of the transition metal precursor to deposit the catalyst precursor.[12]

* Corresponding author. Fax: +49-234-3214115. Tel: +49-234-3228754. E-mail: muhler@techem.ruhr-uni-bochum.de.
[†] Laboratory of Industrial Chemistry, Ruhr University Bochum.
[‡] Fritz Haber Institute of the Max Planck Society.
[§] Lehrstuhl für Physikalische Chemie I, Ruhr University Bochum.
[||] University of Applied Sciences Gelsenkirchen.

(1) Rodriguez, N. M. *J. Mater. Res.* **1993**, *8*, 3233.
(2) Serp, P.; Corrias, M.; Kalck, P. *Appl. Catal. A* **2003**, *253*, 337.
(3) Pham-Huu, C.; Keller, N.; Charbonniere, L. J.; Ziessel, R.; Ledoux, M. J. *Chem. Commun.* **2000**, 1871.
(4) Wang, C.; Waje, M.; Wang, X.; Tang, J. M.; Haddon, R. C.; Yan, Y. *Nano Lett.* **2004**, *4*, 345.
(5) Maksimova, N. I.; Roddatis, V. V.; Mestl, G.; Ledoux, M.; Schloegl, R. *Eurasian Chemico-Technol. J.* **2000**, *2*, 231.
(6) Fan, Y.; Burghard, M.; Kern, K. *Adv. Mater.* **2002**, *14*, 130.
(7) Milewski, J. V. U.S. Patent #3, 580,731, 1971.
(8) (a) Downs, W. B.; Baker, R. T. K. *Carbon* **1991**, *29*, 1173. (b) Downs, W. B.; Baker, R. T. K. *J. Mater. Res.* **1995**, *10*, 625.
(9) McAllister, P.; Wolf, E. E. *Carbon* **1992**, *30*, 189.
(10) Hou, H.; Reneker, D. H. *Adv. Mater.* **2004**, *16*, 69.
(11) Lim, S.; Yoon, S. H.; Shimizu, Y.; Jung, H.; Mochida, I. *Langmuir* **2004**, *20*, 5559.

10.1021/cm051623k CCC: $30.25
Published on Web 10/14/2005

The hydrophobicity of the surface of the VGCFs, however, is a substantial challenge to impregnation techniques, rendering the control of the distribution and morphology of the catalyst particles difficult, especially when the dimensions of the parent fibers decrease to the nanometer range. In addition, the separation of the fibers from the catalyst precursor solution frequently results in entanglement of the fibers. Here, we present the synthesis of nanofibers supported on vapor-grown carbon nanofibers with controlled morphologies and homogeneous distribution by chemical vapor deposition (CVD) and synthesis (CVS): first, the carbon nanofibers were oxygen-functionalized by exposing them to an oxygen plasma. Then, ferrocene was deposited from the gas phase in the presence of oxygen, resulting in CNF-supported FeO_x nanoparticles.[13] Finally, carbon nanobranches were grown by the iron-catalyzed decomposition of cyclohexane.[14] The whole process including the pretreatment is entirely based on well-controlled gas-phase steps, thus fully avoiding wet chemistry:

$$Fe(Cp)_2 \xrightarrow{O_2,CNF} FeO_x/CNF \quad (1)$$

$$C_6H_{12} \xrightarrow{H_2,FeO_x/CNF} CNF/CNF \quad (2)$$

Experimental Section

Carbon nanofibers (Pyrograf III, pyrolytically stripped, diameter 100−200 nm, length 30−100 μm) were obtained from Applied Sciences Inc. The as-grown nanofibers had been pyrolytically stripped by the manufacturer to remove polyaromatic hydrocarbons. The nanofibers received as powder consisting of agglomerates in the range from several micrometers to a few 10 μm were first exposed to a 120 W oxygen plasma for 7 min in a rotating barrel. The plasma-treated nanofibers were used as substrates for the CVD of iron oxides in a fixed-bed reactor with ferrocene (Merck, 98%) as iron source. Nitrogen (purity 99.999%) was used as the carrier gas and synthetic air (20.5% O_2 in N_2) as the oxidizing gas. The flow rates were adjusted by mass flow controllers. The temperature of the sublimation chamber was kept at 110 °C and that of the reaction chamber at 300 °C. In a typical experiment, 0.2 g of plasma-treated nanofibers were loaded into the reactor, and 0.009 g of ferrocene (corresponding to an Fe loading of 1.35 wt %) was placed in the sublimation chamber. The flow rates of both nitrogen and air were 50 mL min^{-1} (STP), resulting in a total flow rate of 100 mL min^{-1}. The deposition was carried out for 3 h, followed by cooling to room temperature to obtain the as-synthesized nanofiber-supported iron oxide composite (FeO_x/CNF). Under these conditions up to 300 °C, the weight loss due to carbon oxidation was found to be negligible.

Subsequently, 0.1 g of Fe-coated nanofibers were placed in a ceramic boat and positioned in a quartz tube reactor (inner diameter 30 mm) and heated to 700 °C at a rate of 10 K min^{-1} in a mixture of hydrogen (purity 99.9999%) and helium (purity 99.9999%) with a volume ratio of 2:1 at a total flow rate of 150 mL min^{-1} (STP). When the mixture was cooled in helium and exposed to air at room temperature at this stage, the sintered FeO_x/CNF nanocomposite was obtained. For the growth of secondary nanofibers at 700 °C, the flow was switched to a saturator filled with cyclohexane and the total flow rate was decreased to 37.5 mL min^{-1} (STP) with the same 2:1 ratio of hydrogen and helium. The duration of the growth of the secondary nanofibers was varied from 5 to 30 min.

The iron loading was determined with a Pye Unicam 7000 ICP-OES spectrometer. The scanning tunneling microscopy (STM) measurements were carried out using a JSPM-4500S ultrahigh vacuum (UHV) combination of a scanning electron microscope (SEM) with a STM (JEOL) operating at a base pressure of 3×10^{-10} mbar. The SEM was operated at electron energies from 0.5 to 12 keV and had a resolution of 7 nm at 12 keV. SEM imaging of the STM tip during an approach allowed us to precisely position the tip on a selected part of the sample within an accessible range of 2 mm × 2 mm. It was possible to operate the STM at temperatures between 50 and 750 K with atomic resolution.[15] X-ray photoelectron spectroscopy (XPS) measurements were carried out in a UHV setup equipped with a Gammadata-Scienta SES 2002 hemispherical analyzer. The base pressure in the measurement chamber was 2×10^{-10} mbar. Monochromatic Al Kα (1486.6 eV; 14 kV; 55 mA) was used as incident radiation. A pass energy of 200 eV and a slit width of 0.2 mm were chosen. The Au foil used for calibration was cleaned by Ar sputtering, and an energy resolution better than 1 eV was achieved. Charging effects were compensated by a flood gun, and binding energies were calibrated using the main C 1s peak at 284.5 eV as internal standard. The morphology and detailed structure of the composites was examined by SEM (LEO Gemini 1530) and transmission electron microscopy (Philips CM 200 FEG). The BET surface area was determined by static nitrogen physisorption at 77 K (Quantachrome Autosorb-1-MP) after outgassing at 573 K until the pressure was lower than 5 mbar.

Results and Discussion

The surface functionalization of carbon nanofibers reported in the literature is based on nitric acid, oxygen plasma, oxidation in air, supercritical fluids, and other methods.[16] Plasma treatment of nanofibers can introduce oxygen-containing functional groups as well as surface defects, which act as anchors for subsequently adsorbed molecules.[17] Plasma treatment as a fast solvent-free technique is advantageous because of the simplicity of operation and the well-controllable process parameters such as power and oxygen partial pressure. The exposure to a 120 W oxygen plasma for 7 min was found to yield the maximum degree of oxygen functionalization required for the anchoring of ferrocene.[18]

During the CVD the ferrocene-loaded carrier gas and air were fed to the reactor simultaneously; i.e., the adsorption of the precursor and its oxidation occurred in one step.[19] Elemental analysis yielded an iron loading of 1.97 wt % after deposition, compared to 1.09 wt % in the as-received nanofibers, where the presence of Fe is due to residues of the iron catalyst used for the nanofiber production. X-ray

(12) Zhu, S.; Su, C. H.; Lehoczky, S. L.; Muntele, I.; Ila, D. *Diamond Relat. Mater.* **2003**, *12*, 1825.
(13) Cheng, J.; Zhang, X.; Liu, F.; Tu, J.; Lu, H.; Sun, Y.; Chen, F. *Mater. Chem. Phys.* **2004**, *87*, 241.
(14) Wang, Y.; Shah, N.; Huffman, G. P. *Catal. Today* **2005**, *99*, 359.
(15) Sato, T.; Kitamura, S.; Iwatsuki, M. *J. Vac. Sci. Technol. A* **2000**, *18*, 960.
(16) (a) Toebes, M. L.; van Heeswijk, J. M. P.; Bitter, J. H.; van Dillen, A. J.; de Jong, K. P. *Carbon* **2004**, *42*, 307. (b) Darmstadt, H.; Roy, C.; Kaliaguine, S.; Ting, J. M.; Alig, R. L. *Carbon* **1998**, *36*, 1183.
(17) Bitter, J. H.; van der Lee, M. K.; Slotboom, A. G. T.; van Dillen, A. J.; de Jong, K. P. *Catal. Lett.* **2003**, *89* 139.
(18) Bubert, H.; Brandl, W.; Kittel, S.; Marginean, G.; Toma, D. *Anal. Bioanal. Chem.* **2002**, *374*, 1237.
(19) Mu, X.; Bartmann, U.; Guraya, M.; Busser, G. W.; Weckenamnn, U.; Fischer, R. A.; Muhler, M. *Appl. Catal. A* **2003**, *248*, 85.

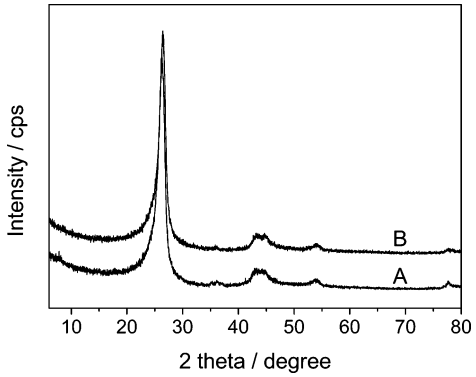

Figure 1. XRD patterns of plasma-treated nanofibers (A) and of the fibers after the chemical vapor deposition of FeO_x (B).

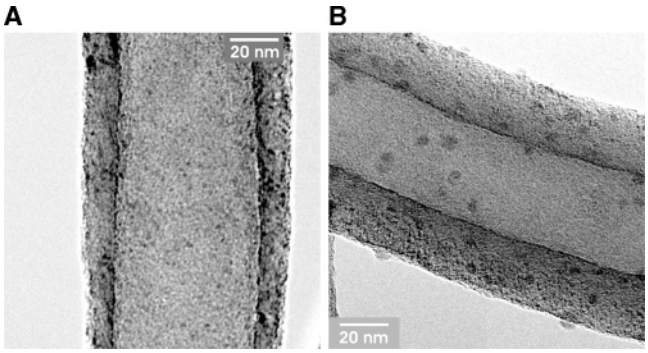

Figure 2. TEM images of iron oxide-coated nanofibers: (A) as-synthesized; (B) heated to 700 °C at a rate of 10 K min^{-1} in a flowing mixture of hydrogen and helium (2:1) followed by transfer in air.

powder diffraction patterns of plasma-treated and Fe-coated nanofibers are shown in Figure 1. No apparent changes were induced by the Fe coating, indicating that the size of the deposited FeO_x particles was below the XRD detection limit of about 2−3 nm. Possible contributions of iron species at around 43.4° and 44.7° 2Θ are obviously originating from the residual iron catalyst (1.09 wt %) in the parent nanofibers. TEM studies provide evidence for the presence of homogeneously distributed particles with diameters of 1−2 nm (Figure 2A).

For the growth of secondary carbon nanofibers from cyclohexane as carbon source, the iron-coated sample was first exposed to a mixture of hydrogen and helium at 700 °C. These reducing conditions led to the formation of metallic iron particles, and the question arises as to whether sintering of the iron particles occurred since the Tammann temperature (one-half of the melting point in Kelvin) was exceeded. The TEM image in Figure 2B shows clearly that the particle size increased significantly up to 5−9 nm. Obviously, larger iron nanoparticles were formed as a result of the coalescence of neighboring particles.[20] The sintering is considered a beneficial effect since iron nanoparticles as small as 1 nm in diameter can hardly catalyze the growth of nanofibers. It is known that the nucleation of the graphene sheets does hardly proceed on metal particles smaller than 5 nm.[21]

STM is an attractive technique for carbon-based catalysts due to its high spatial resolution and the possibility to obtain information on the height of the supported particles.[22] Figure 3A shows a SEM image of a bundle of FeO_x-coated CNFs in the sintered state. By means of SEM a precise positioning of the STM tip on the top of a nanofiber is possible. The STM image (Figure 3B) indicates that there are particles present on the fiber surface. The typical particle diameter is between 5 and 9 nm, in good agreement with the TEM measurements (Figure 2B). Line profiles across the particles are shown in Figure 3C. The highest part reaches about 1.4 nm for larger and 0.5−0.6 nm for smaller particles. The aspect ratio is rather low, even when considering that the particles may be embedded in the carbon surface. Thus, sintering under reducing conditions resulted in an efficient spreading of the iron particles over the carbon surface, presumably assisted by an interfacial layer consisting of iron carbide.

The XP spectra of the as-prepared and sintered iron-coated nanofibers are shown in Figure 4. It has to be noted that the sintered iron sample is also in the oxidized state because of the air exposure during the transfer. The Fe 2p core levels are split into the $2p_{3/2}$ and $2p_{1/2}$ components due to the spin−orbit coupling. The Fe $2p_{3/2}$ core level appears at 711.2 eV, and a shake-up satellite can be observed at 719 eV. Both observations are characteristic for Fe^{3+} species and agree well with Fe_2O_3 literature data,[23] thus confirming the formation of Fe_2O_3 particles during the CVD of ferrocene in the presence of oxygen. No apparent peak shift to lower binding energy was observed for the sintered sample; hence, the presence of metallic iron as well as of Fe^{2+} species can be excluded. Obviously, the tiny metallic iron nanoparticles resulting from the reduction in hydrogen at 700 °C were oxidized completely by air during the sample transfer.

For both samples it was possible to decompose the O 1s spectra into three peaks. The contribution of anionic oxygen in Fe_2O_3 is clearly resolved at 530.2 eV. The peak at 531.8 eV can be attributed mainly to the oxygen-containing functional groups,[24] which were introduced by the oxygen plasma treatment. Most of these groups were removed by heat treatment as indicated by the considerable decrease of the peak intensity (trace 2 in Figure 4B). In addition, OH groups present on Fe_2O_3 originating from the contact with air may also contribute to this peak at 531.8 eV similar to FeOOH.[25] The O 1s peaks at about 533.2 eV can be assigned to adsorbed water on the CNF surface, which was not pumped off in UHV.[26] The C 1s core-level spectra (not shown here) of both samples exhibit a main peak at 284.5 eV due to the graphite-like structure of the CNFs. However, a slight change is observed after the heat treatment in

(20) (a) Ruckenstein, E.; Chen, J. J. *J. Colloid Interface Sci.* **1982**, *86*, 1. (b) Pulvermacher, B.; Ruckenstein, E. *J. Catal.* **1974**, *35*, 115.

(21) (a) de Bokx, P. H.; Kock, A. J. H. M.; Boellaard, E.; Klop, E.; Geus, J. W. *J. Catal.* **1985**, *96*, 468. (b) van den Berg, F. R.; Crajé, M. W. J.; Kooyman, P. J.; van der Kraan, A. M.; Geus, J. W. *Appl. Catal. A* **2002**, *235*, 217.

(22) Atamny, F.; Baiker, A. *Appl. Catal. A* **1998**, *173*, 201.

(23) (a) Muhler, M.; Schloegl, R.; Ertl, G. *J. Catal.* **1992**, *138*, 413. (b) Schedel-Niedrig, Th.; Weiss, W.; Schloegl, R. *Phys. Rev. B* **1995**, *52*, 17449.

(24) Martinez, M. T.; Callejas, M. A.; Benito, A. M.; Cochet, M.; Seeger, T.; Ansón, A.; Schreiber, J.; Gordon, C.; Marhic, C.; Chauvet, O.; Fierro, J. L. G.; Maser, W. K. *Carbon* **2003**, *41*, 2247.

(25) Brundle, C. R.; Chuang, T. J.; Wandelt, K. *Surf. Sci.* **1977**, *68*, 459.

(26) (a) Schloegl, R. In *Handbook of heterogeneous catalysis*; Ertl, G., Knözinger, H., Weitkamp, J., Eds.; Wiley-VCH: Weinheim, 1997; Vol. 1, p 138. (b) Desimoni, E.; Casellas, G. I.; Salvi, A. M.; Castaldi, T. R. I.; Morone, A. *Carbon* **1992**, *30*, 527.

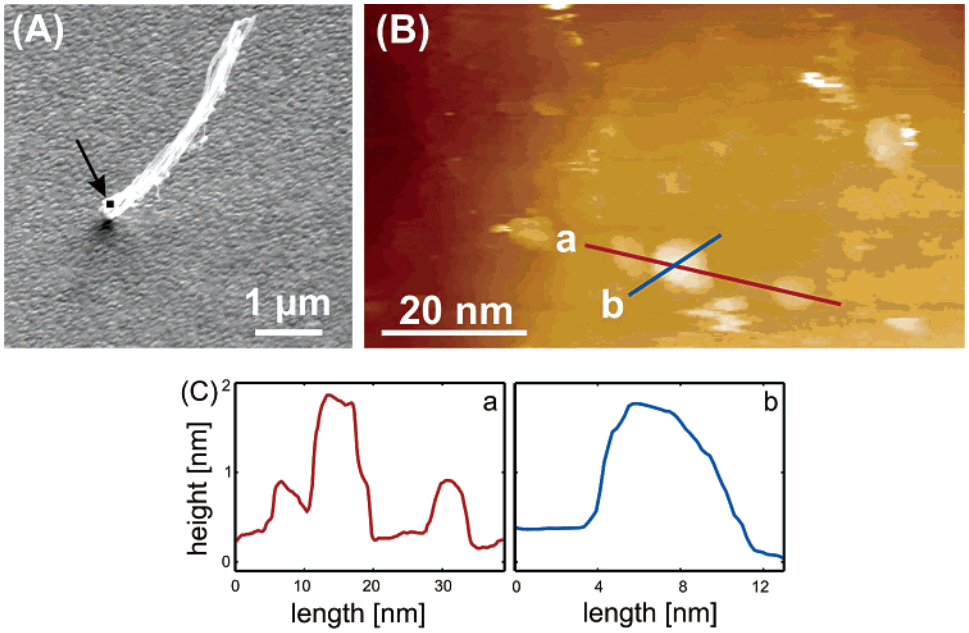

Figure 3. (A) SEM image of a bundle of nanofibers. A typical STM scan area of ~100 nm is roughly marked by a black square and indicated with an arrow; (B) STM image on the surface of an iron oxide-coated nanofiber after heat treatment at 700 °C under a mixture of hydrogen and helium followed by transfer in air (U_{sample} = 700 mV, I = 75 pA); (C) line profiles across the clusters indicated in (B).

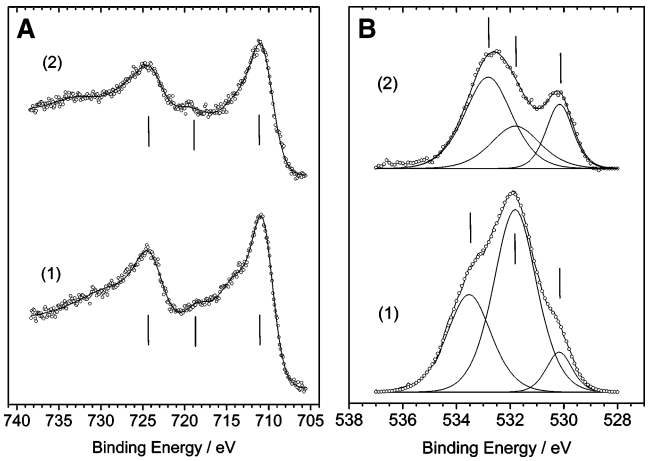

Figure 4. XP Fe 2p (A) and O 1s (B) spectra of iron oxide-coated nanofibers: (1) as-synthesized; (2) heated to 700 °C at a rate of 10 K min^{-1} in flowing hydrogen and helium (2:1) followed by transfer in air. The original data are denoted by circles.

reducing atmosphere: the small peak at about 288.8 eV disappeared, which can be assigned to the carboxyl functional groups.[27] This decomposition during the heat treatment in hydrogen is in good agreement with the decrease of the O 1s component at 531.8 eV observed for the sintered sample. The elemental surface composition of both samples derived from XPS is summarized in Table 1. The surface atomic concentrations of both iron and oxygen decreased considerably after the heat treatment in hydrogen, indicating severe sintering, in agreement with the TEM observations and the loss of oxygen-containing functional groups on the CNF surfaces.

Recently, we showed that the fiber morphology can be tailored by a variety of parameters such as the growth temperature, the time on stream, the composition of the feed

Table 1. Quantitative XPS Results of the Iron Oxide-Coated Carbon Nanofiber Samples in the As-Prepared State and after Heating in Hydrogen and Transfer in Air

sample (FeO_x/CNF)	element	sensitivity factor[32]	surface atomic concentration
as-prepared	C 1s	0.25	86.2%
	O 1s	0.66	11.4%
	Fe 2p	3.0	2.4%
sintered	C 1s	0.25	91.5%
	O 1s	0.66	6.9%
	Fe 2p	3.0	1.6%

gas, and the type and loading of the catalyst.[28] Large catalyst particles usually lead to straight nanofibers and nanotubes,[10] while small particles tend to produce twisted forms with smaller dimensions. The latter, as a consequence, exhibit considerably enhanced specific surface areas. Similarly, all these parameters can be used to tune the growth of secondary filaments on nanofibers based on cyclohexane as the carbon source and the sintered metallic iron nanoparticles as catalysts. Figure 5A shows the plasma-treated nanofibers at low magnification. Figure 5B at high magnification reveals that the Pyrograf III nanofibers exhibit a tubular structure. Figures 5C and 5D, 5E and 5F, and 5G and 5H show the SEM images of the secondary nanofibers on carbon nanofibers grown for 5, 10, and 30 min at low and high magnification, respectively. It can be seen that the nanofibers are distributed homogeneously over the surface of the parent nanofibers. With increasing growth time, the length of the nanofibers increases. In addition, the number of nanofibers per unit surface area of the support fiber increases due to ongoing nucleation of fresh nanofibers. TEM images of the nanofiber−nanofiber composites grown for 30 min are shown

(27) Okpalugo, T. I. T.; Papakonstantinou, P.; Murphy, H.; McLaughlin, J.; Brown, N. M. D. *Carbon* **2005**, *43*, 153.

(28) (a) Schlüter, O. F.-K.; Wehner, B. I.; Hu, D.; Xia, W.; Quandt, T.; Marginean, G.; Brandl, W.; Muhler, M. *Appl. Catal. A* **2004**, *274*, 71. (b) Xia, W.; Schlüter, O. F.-K.; Muhler, M. *Carbon* **2004**, *42*, 2751. (c) Xia, W.; Su, D.; Schloegl, R.; Birkner, A.; Muhler, M. *Adv. Mater.* **2005**, *17*, 1677.

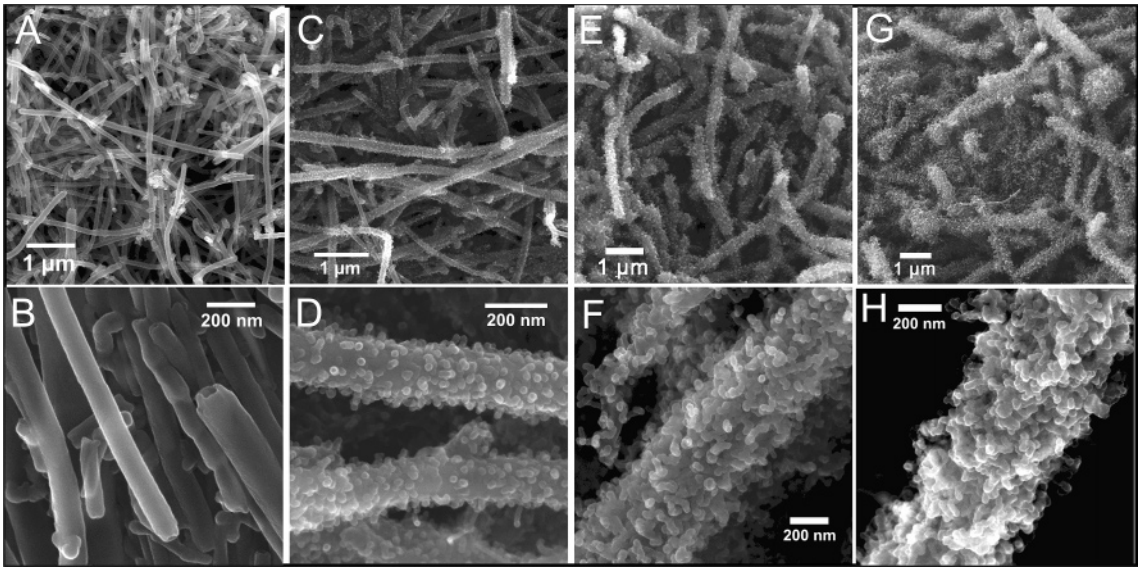

Figure 5. SEM images of plasma-treated Pyrograf III carbon nanofibers (A and B) and nanofibers on nanofibers grown for 5 min (C and D), 10 min (E and F), and 30 min (G and H) at 700 °C from cyclohexane in a mixture of H_2 and He (2:1, total flow rate 37.5 mL min^{-1} (STP)).

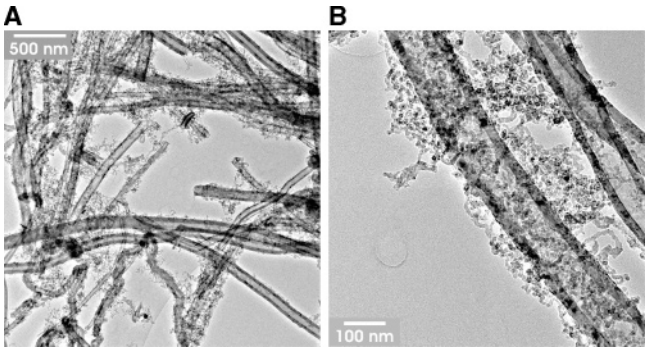

Figure 6. TEM images of nanofiber−nanofiber composites grown for 30 min with (A) lower and (B) higher magnification.

in Figures6A and 6B. The parent and the secondary nanofibers can be clearly distinguished by their dimensions. The observed diameter of the secondary CNFs is in the range from 10 to 20 nm. Obviously, further sintering of the iron particles occurred under growth conditions, resulting in diameters exceeding 10 nm. Longer growth periods result in a slight thickening due to the pyrolytic deposition of amorphous carbon. The iron particles were always found at the tip of the filaments; i.e., the secondary nanofibers originate from the tip-growth mode.

It is reported in the literature that the nanofibers frequently exist in small agglomerated forms.[29] Figure 5A discloses that there are large interfiber voids in the agglomerates, even after the plasma treatment in the rotating barrel. After the growth of the secondary nanofibers, the agglomerates are still intact, but the voids are filled with nanofibers (Figure 5G). An expansion of the total volume of the parent nanofibers due to the growth of the branches was not observed, thus confirming that the nanofibers were grown in the interfiber voids of the parent fibers.

The specific surface area of the as-received nanofibers was in the range from 20 to 30 $m^2\ g^{-1}$, compared to only 10−20 $m^2\ g^{-1}$ for the as-grown nanofibers (technical data of Pyrograf III). The increase in specific surface area originates from the pyrolytic stripping of the as-grown nanofibers applied to remove polyaromatic hydrocarbons.[30] The plasma treatment of the as-received nanofibers increased the specific surface area to 83 $m^2\ g^{-1}$ due to surface roughening and presumably also because of the opening of the inner tube of the nanofibers. After the growth of the secondary nanofibers for 30 min, the specific surface area was found to increase significantly to 205 $m^2\ g^{-1}$. It is worth noting that the specific surface area of the CNF/CNF composites was determined in the as-grown state. An even higher specific surface area can be expected when the thermal treatment or the plasma treatment is additionally performed. Further deposition of noble metal particles such as palladium[31] is planned to be carried out subsequently. In this way, a unique structured hydrogenation catalyst can be obtained. The tailored composite is therefore of great potential as a structured support for carbon-supported catalysts especially in three-phase reactors and in fuel cells.

Conclusion

The carbon nanofiber−nanofiber composite was synthesized by exclusively employing gas-phase reactions. Homogeneously distributed iron oxide nanoparticles were first deposited on functionalized carbon nanofibers by the CVD of ferrocene in the presence of oxygen. Sintering of the nanoparticles was induced under reducing conditions at 700 °C. A decrease of the surface atomic concentrations of iron and oxygen was detected by XPS, and the morphology and the height of the sintered nanoparticles was derived by TEM and STM. Secondary carbon nanofibers were subsequently grown from cyclohexane catalyzed by the sintered iron nanoparticles. It was possible to tune the morphology of the CNF/CNF composite by the process parameters and to achieve a specific surface area of about 200 $m^2\ g^{-1}$.

(29) de Jong, K. P.; Geus, J. W. *Catal. Rev.-Sci. Eng.* **2000**, *42*, 481.

(30) See http://www.apsci.com/ppi-pyro3.html (accessed 2005).

(31) Liang, C.; Xia, W.; Soltani-Ahmadi, H.; Schlüter, O. F.-K.; Fischer, R. A.; Muhler, M. *Chem. Commun.* **2005**, 282.

(32) Briggs, D.; Seah, M. P. *Practical Surface Analysis − 2nd ed.*; John Wiley & Sons: England, 1994; p 635.

Acknowledgment. We are grateful to the MWF/NRW and to DFG (SPP 1119) for financial support. W. Xia thanks the IMPRS of Surface and Interface Engineering in Advanced Materials (SurMat) for a research grant. C. Liang thanks the Alexander von Humboldt foundation for financial support.

CM051623K